Rock Mechanics and Rock Engineering (2021) 54:4369–4378
https://doi.org/10.1007/s00603-021-02502-2

TECHNICAL NOTE

Influence of Cyclic Wetting–Drying on the Shear Strength of Limestone with a Soft Interlayer

Dongming Gu[1,2,3] · Hanlong Liu[1,2] · Xuecheng Gao[1,2] · Da Huang[2] · Wengang Zhang[1,2,3]

Received: 16 August 2020 / Accepted: 4 May 2021 / Published online: 22 May 2021

Keywords Soft interlayer · Wetting–drying cycle · Shear strength · Damage model

1 Introduction

Cyclic wetting–drying can greatly influence rock properties such that a significant decrease in mechanical strength can be expected for a rock undergoing wetting–drying cycles (Zhou et al. 2017; Xie et al. 2018; Gu et al. 2020). The water-weakening effect has been widely recognized to be relevant to many rock failures, typically represented by rockslides in reservoir areas, where rock masses within the riparian zone undergo periodic water-level fluctuations (Huang et al. 2018; Wang et al. 2020). In terms of the long-term instability of rock masses induced by cyclic wetting–drying, the strength degradation of rocks is of major concern (Castellanza et al. 2008). Over the past several decades, a large number of experimental studies have been carried out to investigate the influence of cyclic wetting–drying on the mechanical properties of sandstone (Zhang et al. 2014; Zhao et al. 2017; Yao et al., 2020), shale (Huang et al. 1995), limestone (Beck and Al-Mukhtar 2014), and other types of rock (Mitaritonna et al. 2009; Asahina et al. 2014).

A detailed review of previous studies has revealed that most of the works on this topic focused on exploring the water-weakening behaviors of intact rocks. However, rock masses are typically characterized by joints, soft interlayers, bedding planes and other weak planes (Meng et al. 2017). With their low shear strength and sensitivity to water, weak planes usually play an adverse role on rock stability (Huang et al. 2017). Typical examples of such instabilities include the shear failure of rockslides along natural weak interlayers in reservoir areas (Gu et al. 2017) and fault-related sloughing at underground openings in water-enriched regions (Bruneau et al. 2003; Li et al. 2021). Therefore, it is crucial to evaluate the mechanical properties of weak planes in rock masses under the influence of water. However, due to the difficulties that lie in the preparation of rock specimens with natural discontinuities (specimens are particularly prone to break into two pieces during drilling or polishing procedures), the current experimental research on the water-weakening features of rock discontinuities mainly involves testing on samples with artificial joints (a bare discontinuity or a discontinuity filled with clay/cement mortar to simulate a soft interlayer). For example, Ma et al. (2019) carried out a series of ring shear tests on reconstituted soft interlayers to investigate the influences of the remolded water content on its shear behaviors; Kim and Jeon (2019) investigated the shear characteristics of rock discontinuities under various thermal–hydromechanical conditions by conducting shear tests on rocks with artificial saw-cut surfaces. However, the effect of cyclic wetting–drying on the mechanical behavior of natural rock discontinuities has rarely been reported in the literature.

The main objective of this paper is to investigate the degradation characteristics of the shear strength of rock interlayers due to cyclic wetting and drying. A series of direct shear tests were conducted on rock specimens with a natural soft interlayer. The shear strengths were measured under different normal stresses and different numbers of wetting–drying cycles. The data were then compared to find the trend of the change in shear strength and to establish a predictive relationship between the strength parameters with the number of wetting–drying cycles. Finally, a damage evolution model

✉ Wengang Zhang
cheungwg@126.com

[1] Key Laboratory of New Technology for Construction of Cities in Mountain Area (Chongqing University), Ministry of Education, Chongqing 400045, China

[2] National Joint Engineering Research Center of Geohazards Prevention in the Reservoir Areas, Chongqing 400045, China

[3] School of Civil Engineering, Chongqing University, Chongqing 400045, China

was proposed to describe the relations between the shear parameters and the number of wetting–drying cycles.

2 Characterization of the Tested Material

The material tested is a carbonate rock from Wu Gorge, which is the second gorge of the famous Three Gorges along the Yangtze River (Fig. 1). These rocks, deposited during the Tertiary Period, have two main components: the dominant carbonate matrix and the argillaceous fraction. The former is mainly a relatively homogeneous micritic limestone (host rock, as shown in Figs. 2a and 3), while the latter is present in the form of thin soft interlayers inside the rock. Polarizing microscopy and X-ray diffraction analyses were applied to the crushed rock fractions to identify the mineral phases of the material tested. The results indicate that the host limestone is mainly composed of calcite (99.2%) and that the content of quartz is less than 1% by weight. The main minerals of the soft interlayer are calcite, clay minerals, and quartz, as shown in Fig. 2b and Table 1. The average density of the rock is approximately 2.67 g/cm, and its uniaxial compressive strength (UCS) and Young's modulus are approximately 170 MPa and 11 GPa, respectively.

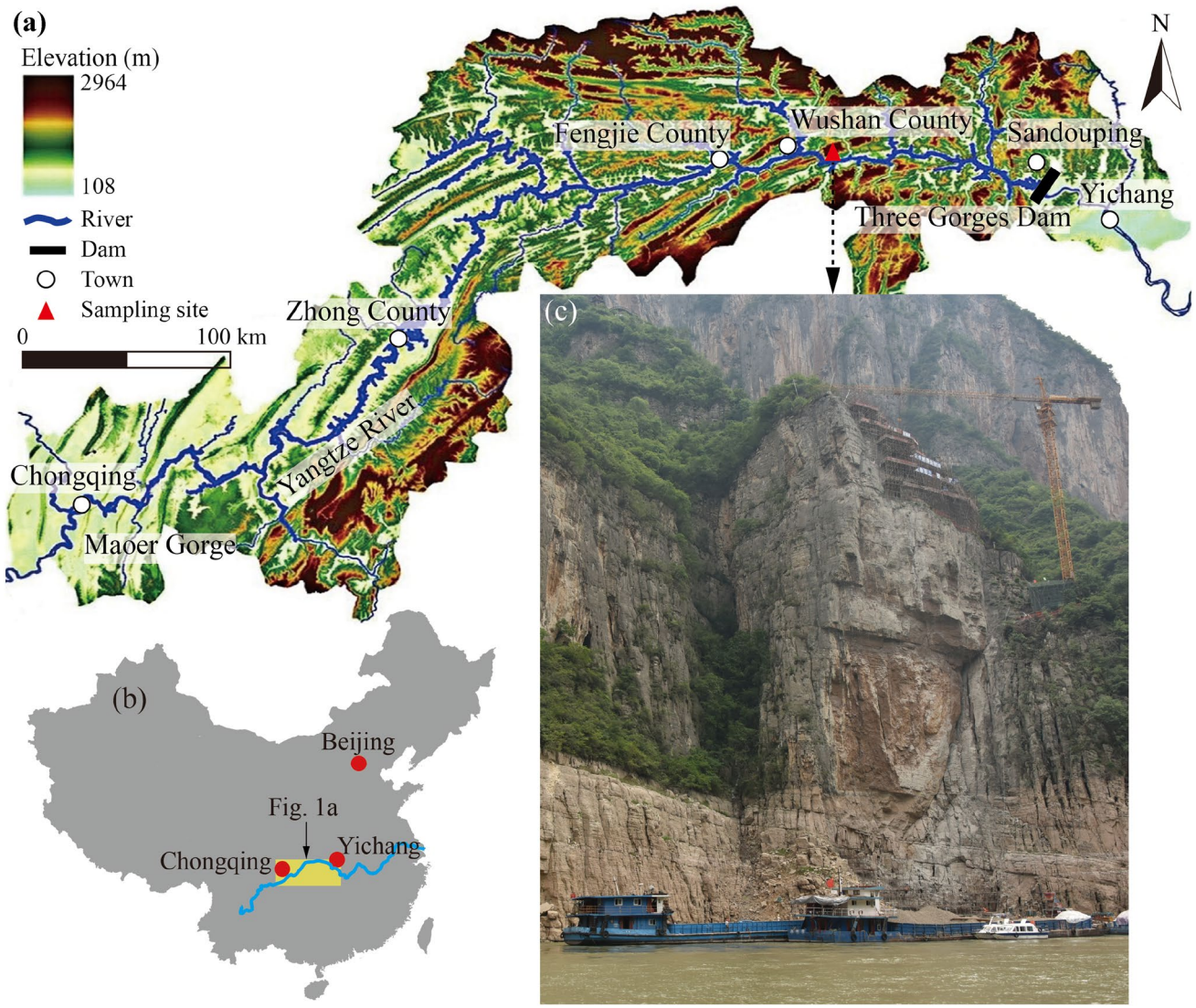

Fig. 1 **a** Detailed location of the Three Gorges Reservoir. **b** Geographic map of the three Gorges reservoir and location of the study area. **c** Site of Jianchuandong

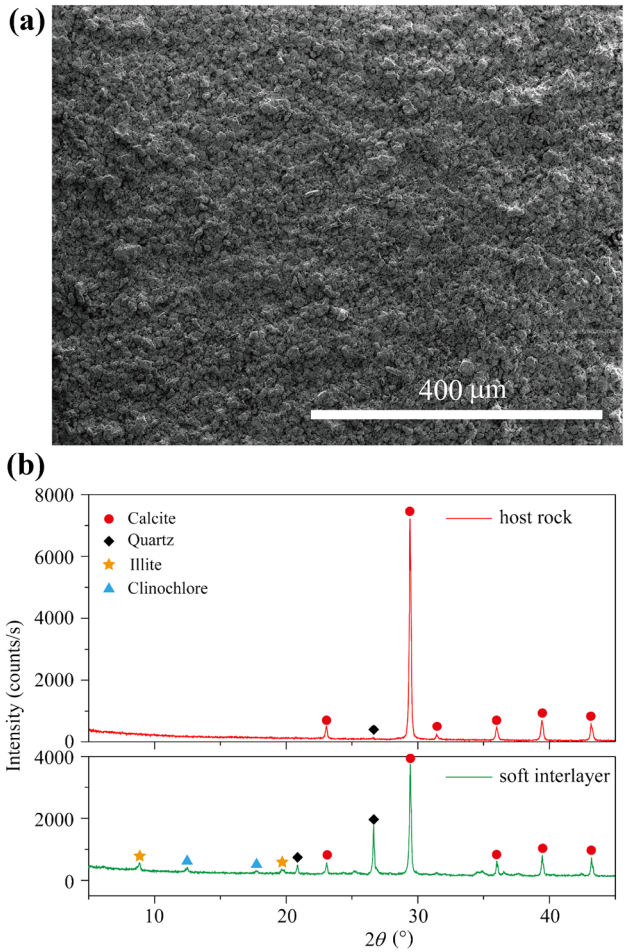

Fig. 2 Microanalysis of the material tested. **a** Micrograph of host rock. **b** X-ray diffraction patterns of host rock and soft interlayer

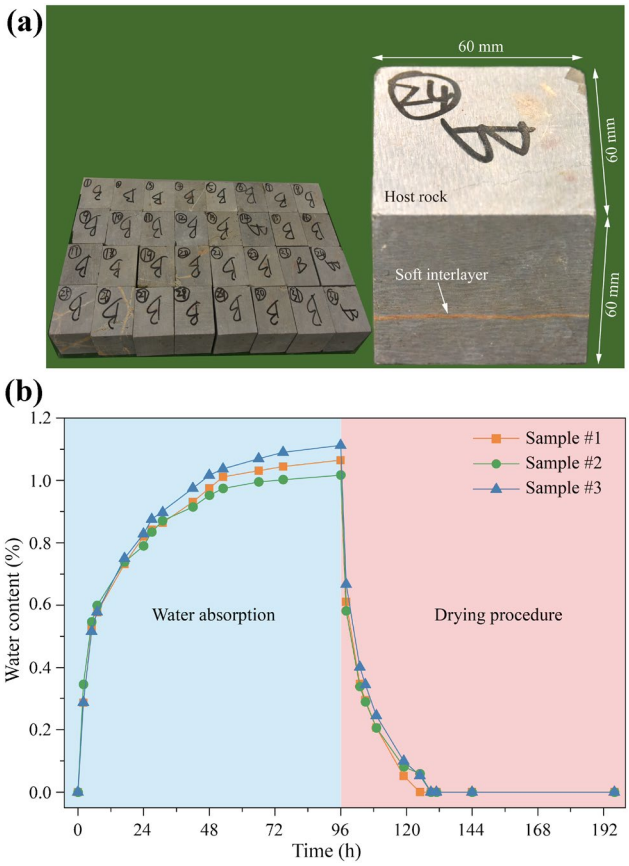

Fig. 3 **a** Part of the samples used in the test. **b** Variation of water content during absorption/drying with time

3 Testing Methodology

3.1 Sample Preparation

Fresh, unweathered rocks dug out at the construction spots (Fig. 1c), which were above the highest reservoir water level, were collected from Jianchuandong in Wu Gorge (Fig. 1). Rock blocks with quasi-flat interlayers were then selected for extracting cubic specimens with a side length of 60 mm (Fig. 3a). All samples were cut so as to make the interlayers near the horizontal and at the half-height of the sample. The six surfaces of the cubic specimens were polished so that the surface roughness is less than 0.02 mm. More than 70 samples were prepared for direct shear tests. The thicknesses of the interlayers of all prepared samples were measured to be within the range of 1–1.5 mm. Then, all the samples were kept in an oven for 120 h at a temperature of 105 °C so that the samples were in a dry state before the subsequent operations.

Table 1 Mineral composition of the rock tested

Mineral composition	Content (%)	
	Limestone	Interlayer
Calcite	99.2	58.2
Clay mineral	–	26.2
Quartz	0.3	14
Other minerals	0.5	1.6

3.2 Water Absorption/Desorption Tests

Water absorption/desorption tests were performed to understand the time-dependent water absorption/desorption process of the rock samples. After the 120 h drying process, three of the rock samples were taken out of the oven, and their masses were measured. Then, the three samples were immersed in a container filled with deionized water at room temperature. Their masses were measured and recorded continuously until no further increase in mass was measured (at this point, the specimens were considered to be saturated). Next, the three saturated samples were placed into the oven.

Similarly, the specimens were also weighed at successive time interval until no variation in their masses was observed. The change in weight was used to determine the rate of water absorption of the specimen at different times, expressed as a percentage of the dry mass of the sample and given as

$$\omega_t = (M_t - M_0)/M_0 \times 100\% \quad (1)$$

where ω_t is the water content of the specimen, M_t is the mass of the sample at time t and M_0 is the mass of the oven-dried sample.

Figure 3b shows the change in water content of the specimens during the saturation and drying processes. It is suggests that a period of 48 h can be considered sufficient to achieve quasi saturation state and that saturated samples can be dried completely after 48 h. Based on these results, in the following testing, a wetting–drying cycle of a rock specimen was performed by submerging the rock in water for 48 h (saturation process) and then drying in an oven at a temperature of 105 °C for another 48 h (drying process).

3.3 Experimental Setup

The tests were performed on a direct shear test system with a loading capacity of 600 kN in both the vertical and horizontal directions. The initial step was placing the sample into the shear cell, controlling the soft interlayer aligned with the shear direction. Then, a normal compressive stress was applied at a loading rate of 0.1 kN/s until a predetermined stress level was reached. Subsequently, the shear force was applied at a constant shear displacement rate of 0.05 mm/min until the sample failed (Ulusay 2014). In this study, the tests were conducted with three different normal compressive stress levels, namely, 20, 40 and 60 MPa, and the number of wetting–drying cycles n was designed to be $n = 0$, 1, 3, 6, 10, and 15. Note that shear tests were carried out both on dry and saturated samples for each operating condition to investigate the influence of cyclic wetting–drying on both the dry and saturated shear strengths of the soft interlayer. Besides, since no undrained measure was taken, the experiments were considered as drained testing for saturated samples.

4 Experimental Results and Analysis

4.1 Changes in Shear Strength Parameters and Corresponding Explanations

Figure 4 shows the typical shear failure surfaces of rock specimens under the saturated and dry conditions. The appearance of exposed failure surfaces clearly tells the state of the specimen: dark brown for saturated state and light yellow for dry state. Besides, the exposed surfaces indicate that failure generally occurs at the interface between rock and soft interlayer. The peak shear stresses and normal stresses acting on the interlayers of the tested rock samples after different numbers of wetting–drying cycles are presented in Table 2 and typical stress–strain curves are illustrated in Fig. 5. It shows that for all samples, after the initial phase, shear stress increased almost linearly with strain up to the maximum and then dropped rapidly, indicating the brittle feature. The cases with normal compressive stress of 20 and 60 MPa were taken as examples to analyze the change in shear strength with the wetting–drying cycles, as shown in Fig. 6. The result shows that, in general, the shear strength of dry sample is higher than that of water-saturated sample when after the same wetting–drying cycles. Shear strengths under both dry and saturated conditions decrease with the increase of wetting–drying cycles. A closer observation of Fig. 6 reveals that the decline trend in saturated strength has slow-down after a treatment of 10 wetting–drying cycles. The result seems to coincide with the findings by Ciantia and Hueckel (2013), who suggested that the rock strength in wet conditions remains about the same after a certain number of wetting–drying cycles, while the dry strength decreases with increasing wetting–drying cycles until reaching the lower bound of wet strength.

The Mohr–Coulomb failure criteria fitting on the points with different numbers of wetting–drying cycles are presented in Fig. 7. Based on the above linear fitting, the shear strength parameters, including the internal frictional angle

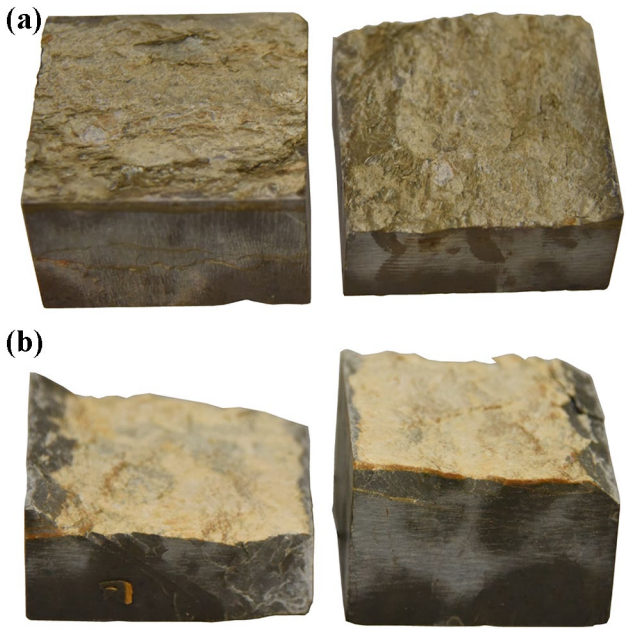

Fig. 4 Typical failure patterns of rock specimens under **a** saturated and **b** dry conditions

Table 2 Peak shear stress (in MPa) of rock joints under different conditions

Number of cycles	$\sigma = 20$ MPa				$\sigma = 40$ MPa				$\sigma = 60$ MPa			
	Saturated		Dry		Saturated		Dry		Saturated		Dry	
0	24.40	26.54	26.77	28.85	31.53	35.11	35.95	37.01	40.70	42.12	49.12	51.02
1	23.51	25.83	25.39	28.34	30.98	34.40	35.46	36.68	38.47	41.05	48.24	50.28
3	21.34	23.24	24.09	24.18	31.15	33.01	34.73	37.95	37.64	42.02	46.43	51.23
6	18.60	21.98	22.77	23.26	28.98	31.02	33.38	35.95	37.52	40.41	44.80	48.85
10	17.62	22.40	19.29	20.87	24.16	26.26	31.99	34.01	35.67	37.64	42.92	43.1
15	17.21	19.04	17.48	18.11	21.95	24.21	30.58	31.66	32.14	34.37	40.54	41.63

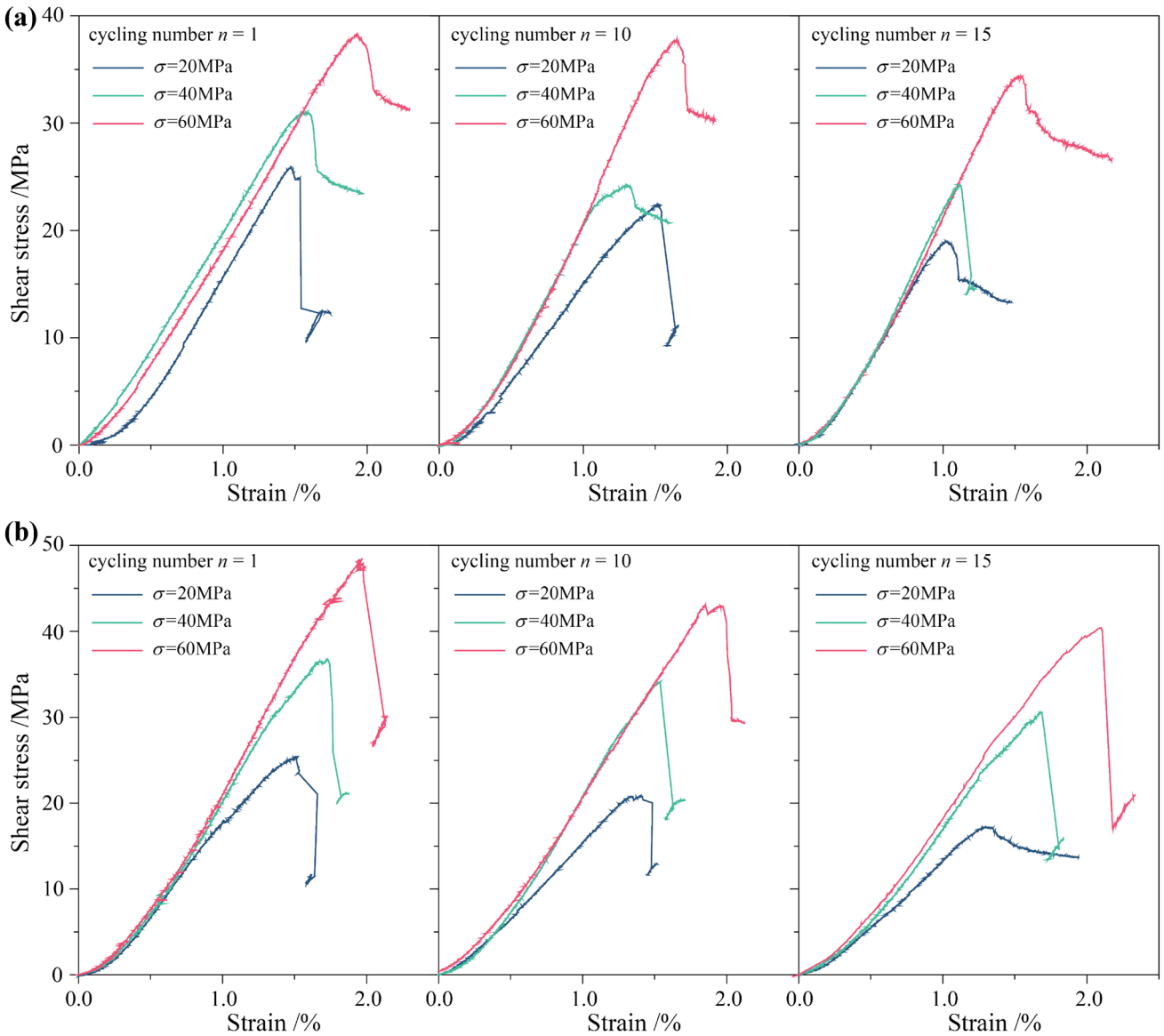

Fig. 5 Typical stress–strain curves of rock specimens under **a** saturated and **b** dry conditions with wetting–drying cycle number of 1, 10, and 15

and cohesion, can be obtained, as shown in Table 3. Note that 0-cycle data represent the samples that did not undergo a wetting-dry cycle. The relationship between the internal frictional angle and the number of wetting–drying cycles under dry and saturated conditions is presented in Fig. 8. It can be seen that the internal frictional angle decreases

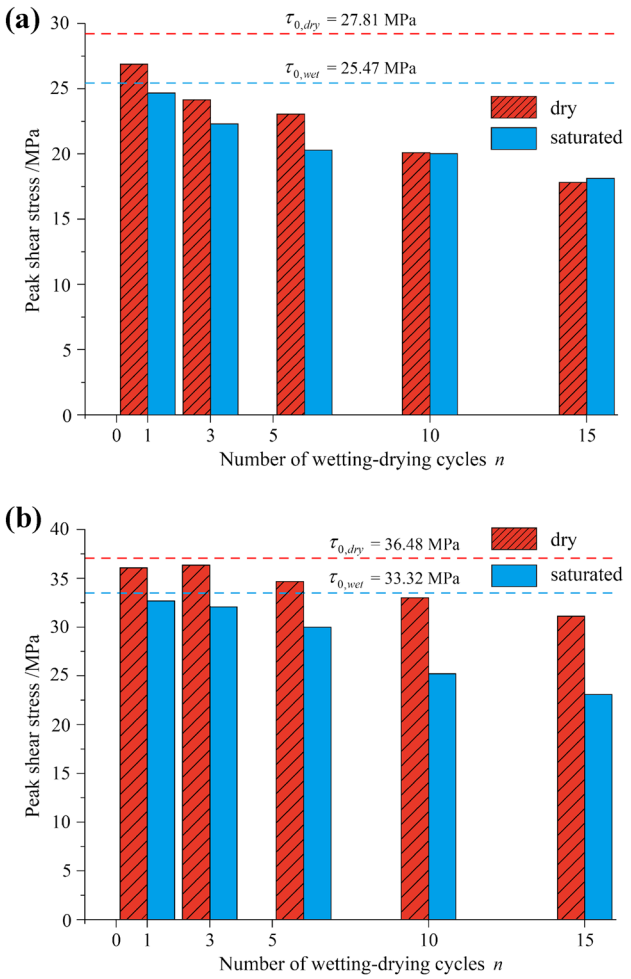

Fig. 6 Change in shear strength with number of wetting–drying cycles under the normal compressive stress of **a** 20 MPa and **b** 40 MPa. ($\tau_{0,dry}$ and $\tau_{0,wet}$ mean the original shear strength in dry and saturated situations, respectively. Note that the average values of data in Table 2 were used)

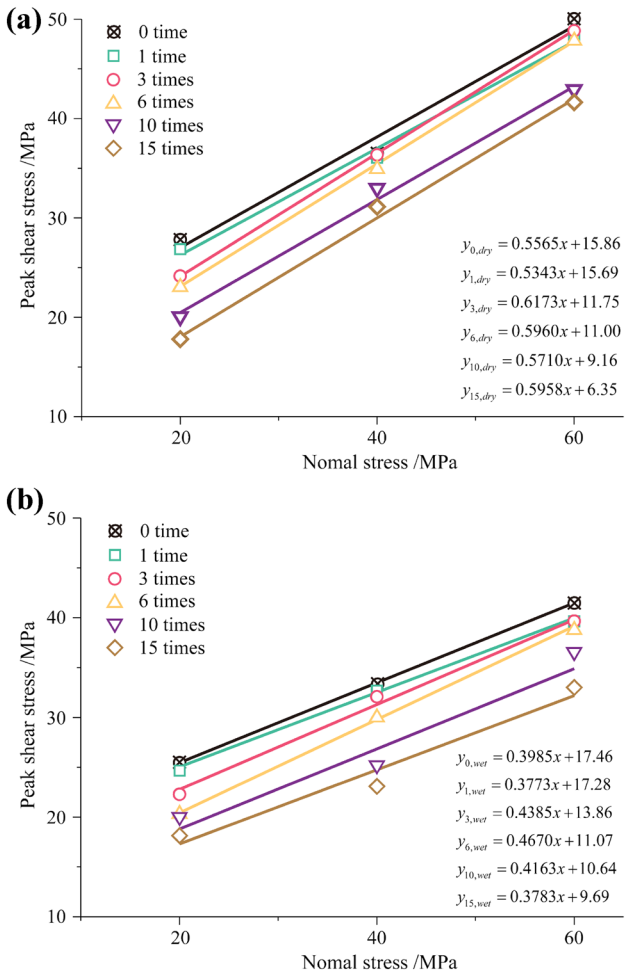

Fig. 7 Relationships between peak shear stress and normal stress for rock interlayers under **a** dry and **b** saturated conditions after different numbers of wetting–drying cycles (the average values of data in Table 2 were used in this figure)

steadily when changing from dry to saturated state, which is consistent with previous experimental studies by other researchers. However, for both the dry and saturated situations, there is no significant correlation between the internal frictional angle of the rock interlayers and the wetting–drying cycles. In other words, the magnitude of the internal frictional angle does not decrease as the number of wetting–drying cycles increase but only fluctuates slightly and irregularly near the average values (Fig. 8), which may be more likely due to the dispersion of the mechanical properties of the rock material.

In both dry and saturated cases, the cohesion gradually decreases with the increase in the number of wetting–drying cycles, as shown in Fig. 9. A closer inspection of the results reveals that the cohesion of the soft interlayer decreases more quickly during the first several cycles: the drop in cohesion after three cycles of wetting–drying

Table 3 Shear strength parameters under different conditions

Number of cycles	Saturated state		Dry state	
	c (MPa)	φ (°)	c (MPa)	φ (°)
0	17.46	21.73	15.86	29.10
1	17.28	20.67	15.69	28.12
3	13.86	23.68	11.75	31.69
6	11.07	25.03	11.00	30.79
10	10.64	22.60	9.16	29.73
15	9.69	20.72	6.35	30.79

corresponds to nearly half of the total reduction in the 15-cycle treatment (43.2 and 46.3% for dry and saturated conditions, respectively). This is more pronounced at saturated situations: the decline of saturated cohesion strength slowing down after 5 wetting–drying cycles, which, once again, seems to corroborate the view that the

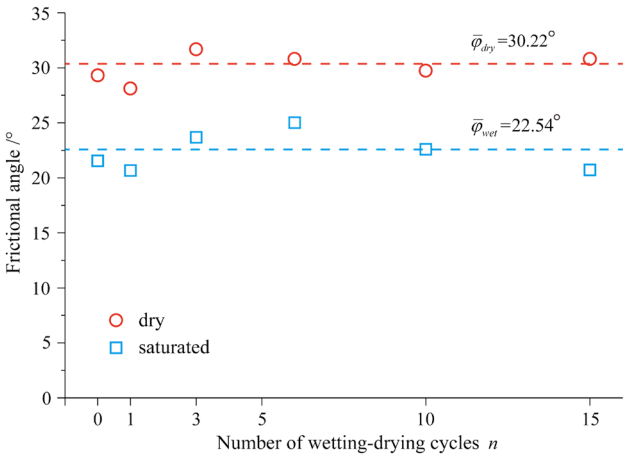

Fig. 8 Relationship between the frictional angle the number of wetting–drying cycles

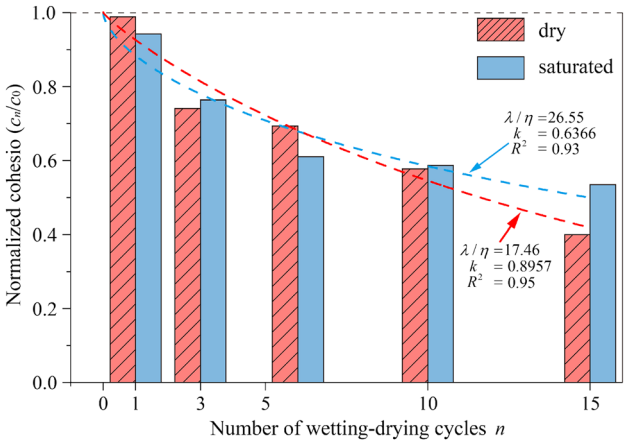

Fig. 9 Changes in normalized cohesion with the number of wetting–drying cycles. (c_0 and c_n are the initial dry/saturated cohesion and cohesion after n wetting–drying cycles, respectively)

saturated strength will remain unchanged after a certain number of wetting–drying cycles. However, it should be noted that the results indicate that the cohesion of the soft interlayers under saturated conditions is higher than that under dry conditions (Table 3), which is contrary to the popular belief that the mechanical properties of rock tend to decrease after water absorption. One possible explanation is that, as rock specimen switching from dry to saturated state, cohesive effect of matric suction (Fredlund and Rahardjo 1993; Thyagaraj and Salini 2015) and adhesive force (Risnes et al. 2005) of the clayey minerals within the interlayer will increase, which leads to a higher cohesion in saturated state.

4.2 Damage Evolution Model

Based on the classical damage theory proposed by Lemaitre (1984), considering the cohesion before the wetting/drying process as the original state and the cohesion after n wetting–drying cycles as the damage state, the damage variable for the cohesion of the rock interlayer (D) can be defined as below:

$$D = 1 - \frac{c_n}{c_0} \tag{2}$$

where c_0 and c_n are the initial cohesion and cohesion after n wetting–drying cycles, respectively. According to Eq. 2, the damage variables for cohesion after different numbers of wetting–drying cycles were obtained and are listed in Table 4. Equation 2 can be rewritten in another form:

$$c_n = c_0(1 - D). \tag{3}$$

Since rock material is composed of micro-units (mineral grains) with different strengths, statistical methods are often used to describe the damage state of micro-units caused by external disturbances, such as stress (Wang et al. 2007), cyclic freezing and thawing (Mu et al. 2017), and cyclic changes in relative humidity (Pineda et al. 2014a; b). Combining Eq. 3 with the statistical damage model (Eq. 4, where E is the elastic modulus, ε is the elastic strain, N_f is the number of already failed micro-units and N is the original number of micro-units) proposed by Krajcinovic and Silva (1982), the following expression was obtained:

$$\sigma = E\varepsilon\left(1 - \frac{N_f}{N}\right). \tag{4}$$

The damage variable D can be defined as a ratio of N_f and N, expressed as follows:

$$D = \frac{N_f}{N}. \tag{5}$$

Table 4 Damage variables for cohesion of interlayers after different wetting–drying cycles

Number of cycles	Saturated state $D_{c,\mathrm{wet}}$	Dry state $D_{c,\mathrm{dry}}$
0	0.00	0.00
1	0.01	0.01
3	0.21	0.26
6	0.37	0.31
10	0.39	0.42
15	0.45	0.60

Considering that at the micro-view, a micro-unit in rock disintegrates when its shrinkage–expansion strain caused by wetting–drying cycles exceeds the threshold level (as shown in Fig. 6c), the damage state of the micro-unit can be viewed as closely relevant to its micro strain. We assumed that the damage probability density function for micro-units caused by micro strain ε due to wetting–drying cycles is $p(\varepsilon)$. Then, the damage variable can be expressed as follows:

$$D = \frac{\int Np(\varepsilon)d\varepsilon}{N} \tag{6}$$

The Weibull distribution, which is commonly used in structural failure applications (Lu et al. 2002; Seal and Sherry 2016; Zhang et al. 2020), was used to describe the micro-damage in this study. Therefore, the strain probability density function becomes as following:

$$p(\varepsilon) = \frac{k}{\lambda}\left(\frac{\varepsilon}{\lambda}\right)^{k-1}\exp\left[-\left(\frac{\varepsilon}{\lambda}\right)^{k}\right] \tag{7}$$

where k and λ are the shape and scale parameters, respectively. Combining Eqs. 6 and 7, the damage variable D based on the Weibull distribution can be obtained:

$$D = 1 - \exp\left[-\left(\frac{\varepsilon}{\lambda}\right)^{k}\right]. \tag{8}$$

According to Eq. 8, the relationship between the damage variable D and the micro strain ε during wetting–drying cycles was obtained. However, in the practical use of Eq. 8, it is difficult to determine the value of the micro strain ε. As an alternative, we assumed that the micro strain ε follows a linear relationship with the number of wetting–drying cycles n:

$$\varepsilon = \eta n \tag{9}$$

where η is a linear fitting coefficient. Substituting Eq. 9 into Eq. 8, results in the following expression:

$$D = 1 - \exp\left[-\left(\frac{\eta n}{\lambda}\right)^{k}\right]. \tag{10}$$

Combining Eqs. 3 and 10, we can obtain the strength degradation model of cohesion of rock interlayers:

$$\frac{c_n}{c_0} = \exp\left[-\left(\frac{\eta n}{\lambda}\right)^{k}\right] = \exp\left[-\left(\frac{n}{\lambda/\eta}\right)^{k}\right] \tag{11}$$

where c_0 and c_n are the initial cohesion and cohesion after n wetting–drying cycles, respectively; n represents the number of wetting–drying cycles; and k and λ/η can be viewed as the shape and scale parameters in the Weibull distribution. The testing results in Table 3 were used to fit the power relationship of Eq. 11. The values of the shape parameter k and scale parameter λ/η were then obtained, as shown in Fig. 9. Plugging Eq. 11 into the Mohr–Coulomb strength criterion, we obtained the damage evolution law for the shear strength of the rock interlayer during wetting–drying cycles:

For the dry state:

$$\begin{aligned}\tau_{n,\mathrm{dry}} &= c_{0,\mathrm{dry}}\left(1 - D_{n,\mathrm{dry}}\right) + \sigma\tan\left(\overline{\phi}_{\mathrm{dry}}\right)\\ D_{n,\mathrm{dry}} &= 1 - \exp\left[-\left(\frac{n}{\lambda/\eta}\right)^{k}\right], \quad (\lambda/\eta = 17.46, k = 0.8957).\end{aligned} \tag{12}$$

For the saturated state:

$$\begin{aligned}\tau_{n,\mathrm{wet}} &= c_{0,\mathrm{wet}}\left(1 - D_{n,\mathrm{wet}}\right) + \sigma\tan\left(\overline{\phi}_{\mathrm{wet}}\right)\\ D_{n,\mathrm{wet}} &= 1 - \exp\left[-\left(\frac{n}{\lambda/\eta}\right)^{k}\right], \quad (\lambda/\eta = 26.55, k = 0.6366)\end{aligned} \tag{13}$$

where the subscript n denotes the number of wetting–drying cycles, and the subscript dry/wet represents the dry/saturated state, τ is the shear strength of the interlayer, σ is the applied normal stress, c_0 is the original cohesion, $\overline{\phi}$ is the average internal frictional angle, and D represents the damage variable.

A detailed comparison of the shear strength between the experimental results and the estimated values based on the damage evolution model is listed in Table 5. The relative errors of this method are less than 10%, which suggests that the proposed model is capable of estimating the shear strength of rock interlayers subjected to wetting–drying cycles.

5 Limitation and Discussion

It should be noted that there are a few factors that limit the generalization of the findings made in this study. For starters, in the drying process, to speed up the drying process, a temperature of 105 °C was adopted, which is generally considered too high and may cause damages to clayey materials. A gentle temperature, such as 60 °C, is recommended in the future tests. Second, considering the high-stress geologic setting of the study area, the vertical stresses applied in the direct shear tests were set at high levels. The corresponding results were evaluated using the linear Mohr–Coulomb criterion, which is believed to work well at low stress levels. However, it is known that the shear strength envelope for rock is highly nonlinear, especially at low stress levels. The present study lacks the results of direct shear tests performed at low stress levels. It is suspected these may be the causes of higher cohesions in saturated state. In future studies, direct shear tests at low stress levels should be carried out, and

Table 5 Comparison of the shear strengths between the experimental results (average values in Table 2) and the estimated values based on the damage evolution model

Number of cycles	$\sigma = 20$ MPa		$\sigma = 40$ MPa		$\sigma = 60$ MPa	
	Saturated	Dry	Saturated	Dry	Saturated	Dry
0	25.47–25.76 (1%)	27.81–27.51 (1%)	33.32–34.06 (2%)	36.48–39.16 (7%)	41.41–42.36 (2%)	50.07–50.81 (2%)
1	24.67–23.72 (4%)	26.87–26.33 (2%)	32.69–32.03 (2%)	36.07–37.98 (5%)	39.76–40.33 (1%)	49.26–49.63 (1%)
3	22.29–21.90 (2%)	24.14–24.55 (2%)	32.08–30.21 (6%)	36.34–36.20 (1%)	39.83–38.51 (3%)	48.83–47.85 (2%)
6	20.29–20.15 (1%)	23.02–22.45 (3%)	30–28.45 (5%)	34.67–34.10 (2%)	38.97–36.75 (6%)	46.83–45.75 (2%)
10	20.01–18.51 (8%)	20.08–20.29 (1%)	25.21–26.81 (6%)	33–31.94 (3%)	36.66–35.11 (4%)	43.01–43.59 (1%)
15	18.13–17.01 (6%)	17.8–18.28 (3%)	23.08–25.31 (10%)	33.26–33.61 (1%)	31.12–29.93 (4%)	41.09–41.57 (1%)

Data in the table are in the form of "experimental result-estimated value (error)"

a more complicated criterion may be used to evaluate the shear strength of rock interlayers at both high and low stress levels. Other reasons such as the clayey matrix of the interlayer being only partially saturated may also lead to higher cohesions in saturated state. Microscopic analysis (such as XRD and SEM) on the change of the clayey fraction during wetting–drying cycles may help clarify this issue. Last but not least, we assumed that the relationship between the strain and the number of wetting–drying cycles was linear when deducing the damage evolution model. However, it has been suggested that rock subjected to cyclic wetting–drying displays finite damage deformation, after which no further damage strain is caused by the application of additional cycles. In other words, the relationship between the strain and the number of wetting–drying cycles may only be linear at a low number of cycles, which means our testing results and the proposed degradation model are valid for only a limited number of wetting–drying cycles.

6 Conclusions

The mechanical weakening of sedimentary rocks induced by wetting–drying cycles is a well-known and extensively characterized phenomenon. Many experimental studies have been reported on the mechanical behaviors of intact sedimentary rocks under wetting–drying cycles. However, weak interlayers, which are widespread geological component in rock masses, have a significant influence on the strength of rock masses. Their water-weakening behaviors have not been clearly identified and quantified. In this paper, the shear behaviors of natural rock interlayers under wetting–drying cycles were investigated by conducting direct shear tests. The main conclusions are as follows:

1. In general, the shear strength of dry sample is higher than that of water-saturated sample when after the same wetting–drying cycles. Both the saturated and dry strengths of rock interlayers decrease with increasing wetting–drying cycles. Distinguishingly, the decline trend in saturated strength will slow-down after a certain number of wetting–drying cycles.
2. The two Mohr–Coulomb shear strength parameters, i.e., internal frictional angle and cohesion, present different variation characteristics and sensitivities to the number of wetting–drying cycles: the magnitude of the internal frictional angle fluctuates slightly and irregularly near its average level with an increasing number of wetting–drying cycles, while the cohesion shows a clear nonlinear decreasing trend as the number of wetting–drying cycles increases.
3. A damage evolution model incorporating the influence of wetting–drying cycles was developed to describe the degradation characteristics of the rock interlayer with an increasing number of wetting–drying cycles. It can be used to estimate the shear strength of the rock interlayer during the cyclic process of wetting–drying.

This study can contribute to a better understanding of the mechanism of the variations in shear characteristics under cyclic wetting–drying conditions. Additionally, the results can be used to assess the stability of discontinuous rock structures, where the effect of wetting–drying cycles should be considered.

Acknowledgements This work is supported by the National Natural Science Foundation of China (No. 41902270), Chongqing Postdoctoral Science Foundation (cstc2019jcyj-bshX0032), Open foundation of State Key Laboratory of Geohazard Prevention and Geoenvironmental Protection (SKLGP2020K025).

References

Asahina D, Houseworth JE, Birkholzer JT, Rutqvist J, Bolander JE (2014) Hydro-mechanical model for wetting/drying and fracture development in geomaterials. Comput Geosci 65:13–23

Beck K, Al-Mukhtar M (2014) Cyclic wetting-drying ageing test and patina formation on tuffeau limestone. Environ Earth Sci 71:2361–2372

Bruneau G, Tyler DB, Hadjigeorgiou J, Potvin Y (2003) Influence of faulting on a mine shaft—a case study: Part i—background and instrumentation. Int J Rock Mech Min 40:95–111

Castellanza R, Gerolymatou E, Nova R (2008) An attempt to predict the failure time of abandoned mine pillars. Rock Mech Rock Eng 41:377–401

Ciantia MO, Hueckel T (2013) Weathering of submerged stressed calcarenites: chemo-mechanical coupling mechanisms. Geotechnique 63(9):768–785

Fredlund DG, Rahardjo H (1993) Soil mechanics for unsaturated soils. Wiley, New York

Gu DM, Huang D, Yang WD, Zhu JL, Fu GY (2017) Understanding the triggering mechanism and possible kinematic evolution of a reactivated landslide in the three gorges reservoir. Landslides 14:2073–2087

Gu DM, Huang D, Zhang WG, Gao XC, Yang C (2020) A 2d dem-based approach for modeling water-induced degradation of carbonate rock. Int J Rock Mech Min 126:104188

Huang SL, Speck RC, Wang Z (1995) The temperature effect on swelling of shales under cyclic wetting and drying. Int J Rock Mech Min Sci Geomech Abstr 32:227–236

Huang MS, Fan XP, Wang HR (2017) Three-dimensional upper bound stability analysis of slopes with weak interlayer based on rotational-translational mechanisms. Eng Geol 223:82–91

Huang D, Gu DM, Song YX, Cen DF, Zeng B (2018) Towards a complete understanding of the triggering mechanism of a large reactivated landslide in the three gorges reservoir. Eng Geol 238:36–51

Kim T, Jeon S (2019) Experimental study on shear behavior of a rock discontinuity under various thermal, hydraulic and mechanical conditions. Rock Mech Rock Eng 52:2207–2226

Krajcinovic D, Silva MAG (1982) Statistical aspects of the continuous damage theory. Int J Solids Struct 18:551–562

Lemaitre J (1984) How to use damage mechanics. Nucl Eng Des 80:233–245

Li A, Dai F, Liu Y, Du HB, Jiang RC (2021) Dynamic stability evaluation of underground cavern sidewalls against flexural toppling considering excavation-induced damage. Tunn Undergr Space Technol 112:103903

Lu CS, Danzer R, Fischer FD (2002) Fracture statistics of brittle materials: Weibull or normal distribution. Phys Rev E 65:067102

Ma C, Zhan HB, Zhang T, Yao WM (2019) Investigation on shear behavior of soft interlayers by ring shear tests. Eng Geol 254:34–42

Meng FZ, Zhou H, Wang ZQ, Zhang LM, Kong L, Li SJ, Zhang CQ (2017) Influences of shear history and infilling on the mechanical characteristics and acoustic emissions of joints. Rock Mech Rock Eng 50:2039–2057

Mitaritonna G, Pineda J, Arroyo M, Romero E (2009) The effect of drying-wetting cycles on the seismic properties of an anisotropic claystone. In: Poro-Mechanics Iv, pp 286–293

Mu JQ, Pei XJ, Huang RQ, Rengers N, Zou XQ (2017) Degradation characteristics of shear strength of joints in three rock types due to cyclic freezing and thawing. Cold Reg Sci Technol 138:91–97

Pineda JA, Romero E, DE Gracia M, Sheng D (2014a) Shear strength degradation in claystones due to environmental effects. Géotechnique 64(6):493–501

Pineda JA, Alonso EE, Romero E (2014b) Environmental degradation of claystones. Géotechnique 64(1):64–82

Risnes R, Madland MV, Hole M, Kwabiah NK (2005) Water weakening of chalk—mechanical effects of water-glycol mixtures. J Petrol Sci Eng 48:21–36

Seal CK, Sherry AH (2016) Weibull distribution of brittle failures in the transition region. In: 21st European Conference on Fracture, (Ecf21) vol 2, pp 1668–1675

Thyagaraj T, Salini U (2015) Effect of pore fluid osmotic suction on matric and total suctions of compacted clay. Geotechnique 65:952–960

Ulusay R (2014) The ISRM suggested methods for rock characterization, testing and monitoring: 2007–2014. Springer International Publishing, Switzerland

Wang ZL, Li YC, Wang JG (2007) A damage-softening statistical constitutive model considering rock residual strength. Comput Geosci 33:1–9

Wang L, Yin Y, Huang B, Dai Z (2020) Damage evolution and stability analysis of the Jianchuandong dangerous rock mass in the three Gorges Reservoir Area. Eng Geol 265:105439

Xie KN, Jiang DY, Sun ZG, Chen J, Zhang WG, Jiang X (2018) Nmr, mri and ae statistical study of damage due to a low number of wetting-drying cycles in sandstone from the three gorges reservoir area. Rock Mech Rock Eng 51:3625–3634

Yao W, Li C, Zhan H, Zhou JQ, Criss RE, Xiong S, Jiang X (2020) Multiscale study of physical and mechanical properties of sandstone in three gorges reservoir region subjected to cyclic wetting-drying of yangtze river water. Rock Mech Rock Eng 53(5):2215–2231

Zhang ZH, Jiang QH, Zhou CB, Liu XT (2014) Strength and failure characteristics of jurassic red-bed sandstone under cyclic wetting-drying conditions. Geophys J Int 198:1034–1044

Zhang H, Wang ZZ, Ruan BT, Li ZC, Zhao WC, Ranjith PG, Wang TT (2020) A brittleness evaluation method of rock constitutive relationship with weibull distribution based on double-body system theory. Energy Sci Eng 8:3333–3347

Zhao ZH, Yang J, Zhang DF, Peng H (2017) Effects of wetting and cyclic wetting-drying on tensile strength of sandstone with a low clay mineral content. Rock Mech Rock Eng 50:485–491

Zhou Z, Cai X, Chen L, Cao WH, Zhao Y, Xiong C (2017) Influence of cyclic wetting and drying on physical and dynamic compressive properties of sandstone. Eng Geol 220:1–12